PCCP

An evaluation of solvent effects and ethanol oxidation

Journal:	*Physical Chemistry Chemical Physics*
Manuscript ID	CP-ART-02-2021-000630.R3
Article Type:	Paper
Date Submitted by the Author:	01-Jul-2021
Complete List of Authors:	Mei, Yuhan; Worcester Polytechnic Institute, Chemical Engineering Deskins, Nathaniel; Worcester Polytechnic Institute, Chemical Engineering

PCCP

ARTICLE TYPE

Cite this: DOI: 00.0000/xxxxxxxxxx

An evaluation of solvent effects and ethanol oxidation

Yuhan Mei and N. Aaron Deskins

Received Date
Accepted Date

DOI: 00.0000/xxxxxxxxxx

Understanding liquid-metal interfaces in catalysis is important, as the liquid can speed up surface reactions, increase the selectivity of products, and open up new favorable reaction pathways. In this work we modeled using density functional theory various steps in ethanol oxidation/decomposition over Rh(111). We considered implicit (continuum), explicit, and hybrid (implicit combined with explicit) solvation approaches, as well as two solvents, water and ethanol. We focused on modeling adsorption steps, as well as C-C/C-H bond scission and C-O bond formation reactions. Implicit solvation had very little effect on adsorption and reaction free energies. However, using the explicit and hybrid models, some free energies changed significantly. Furthermore, ethanol solvent had a more considerable impact than water solvent. We observed that preferred reaction pathways for C-C scission changed depending on the solvation model and solvent choice (ethanol or water). We also applied the bond-additivity solvation method to calculate heats of adsorption. Heats of adsorption and reaction using the bond-additivity model followed the same trends as the other solvation models, but were ∼1.1 eV more endothermic. Our work highlights how different solvation approaches can influence analysis of the oxidation/decomposition of organic surface species.

1 Introduction

Fuel cells can generate electricity directly from fuels, being much more efficient than conventional electricity production involving combustion[1,2]. Several types of fuel cells exist, and the direct ethanol fuel cell uses ethanol as a fuel. Ethanol is an attractive choice because it is less toxic than other fuels, and has a high energy density.[3,4]. Furthermore, ethanol can be considered a renewable fuel source because it can be produced from agricultural bioprocesses[5,6].

Ethanol oxidation is a crucial reaction at the anode in direct ethanol fuel cells, typically involving metal catalysts[6–16]. A related reaction is ethanol decomposition, which is involved for example in ethanol steam reforming[17]. The study of ethanol decomposition can provide insight into ethanol oxidation and, therefore, has been extensively studied[18–21]. Complete oxidation of ethanol, which maximizes electricity production, involves facile C-H and C-C bond breaking to form CO_2 as a final product. Unfortunately, incomplete oxidation occurs when using many catalysts due to slow C-C kinetics, and products like acetaldehyde and acetic acid are formed. A scientific approach to developing new ethanol oxidation catalysts requires a better understanding of the fundamental chemical processes at the catalyst surface, including how liquid-solid interfaces may affect such chemical processes. Indeed, solvent effects can be significant for reactions involving metal catalysts[22–24]. For instance, recent work[25] showed that an ethanol solvent (as opposed to the typical water solvent) may enable room-temperature ethanol oxidation. Changing the solvent may be one way to tune the ethanol oxidation reaction to obtain better catalyst activity, but better characterization of solvent effects are needed.

For molecular modeling simulations, particularly density functional theory (DFT), several types of solvation approaches exist. Implicit solvation techniques represent the solvent as a continuum surrounding solute atoms. This approach adds little increased time to the simulation. Recent developments, such as VASPsol[26,27], add implicit modeling capability to periodic DFT calculations when modeling surfaces. Furthermore, Heyden and colleagues developed the iSMS method[28], which obtains solvation energies from metal cluster calculations using, for instance, the COSMO solvation model[29]. However, it is unclear if such implicit solvation techniques may fully describe solvation effects. In our previous work[30], we assessed implicit solvation over the Pt(111) surface. Adsorption of many common adsorbates and four reactions were modeled in both vacuum and implicit water. The results showed that the presence of water could significantly change some species' adsorption energies. However, the implicit solvation model may not always be able to describe hydrogen bonding correctly.

Explicit solvation includes solvent molecules directly as part of the simulation. For instance, water molecules may be modeled

Department of Chemical Engineering, Worcester Polytechnic Institute, 100 Institute Road, Worcester, Massachusetts 01609, USA

† Electronic Supplementary Information (ESI) available: [details of any supplementary information available should be included here]. See DOI: 10.1039/cXCP00000x/

along with reaction intermediates over the catalyst surface. Several catalytic studies have been performed using explicit solvation[31–36]. While explicit solvation approaches are, in principle, more robust than implicit solvation approaches, the downside to explicit solvation is that the computational time and complexity increase as more molecules are added to the simulation. There are several ways to perform explicit solvation calculations. The ab initio Molecular Dynamics (AIMD) approach has been used to describe the complex structures that may arise at liquid-solid interfaces.[37,38] Getman and colleagues[32,33] have used empirical molecular dynamics simulations to generate solvent-metal structures that were then modeled using DFT. Heyden and his group[36] have reported on a hybrid QM/MM methodology, named eSMS (Explicit Solvation for Metal Surfaces). A simple method involves adding solvent molecules and allowing geometry relaxation.

A third approach combines implicit and explicit solvation (a hybrid approach) to include solvent molecules while also applying implicit solvation. Such an approach can, in principle, be much faster than explicit solvation schemes involving many molecules, but may also improve upon the accuracy of implicit solvation. The cluster-continuum model (CCM) was reported by Pliego et al.[39], which combines implicit solvation with a finite number of explicit water molecules (a cluster). In their work, CCM was demonstrated to be more accurate than implicit continuum solvation models for studying chemical reactions in the liquid phase. Wang's group[40] also utilized the hybrid method to simulate water solvation for formic acid oxidation over Pt(111) surfaces. Schweitzer et al.[20] investigated solvation and alcohol decomposition over Pt using a hybrid model. They placed an explicit water molecule, while applying implicit solvation, on the Pt surface arranged to interact with the oxygen atom of the adsorbate, forming a hydrogen bond. When applying their hybrid model O-H and C-OH bond scission became more exothermic, while C-H and C-C bond scission became more endothermic.

There have been numerous DFT studies of ethanol oxidation over metal surfaces[18,41–45], but these have largely been performed in vacuum, many ignoring the liquid-metal interface. However, there has been some modeling work examining ethanol decomposition in the presence of solvent. Gu et al.[46] used an implicit model to investigate the impact of water on ethanol scission reactions over Pt(111). Schweitzer and colleagues[20] used a hybrid model to investigate bond breaking in alcohol decomposition at the H_2O/Pt(111) interface. Still, questions regarding appropriate robust solvation models exist. These previous papers used only the implicit method or only one water molecule when applying the explicit model. According to the work of Gu et al. and Schweitzer et al., the implicit solvation method had minimal impact on C-C and C-H bond breaking energies, and it is unclear if one explicit water molecule is sufficient to describe solvation effects.

Furthermore, even though water solvation have been applied to ethanol oxidation, the impact of other solvents (like ethanol) is still unclear. In previous work, water was widely studied as a solvent, but other solvents, like ethanol, may also be important. Michel et al.[34] modeled C-H and O-H bond dissociation of ethanol over the Rh(111) surface with an extra ethanol molecule or water molecule pre-adsorbed to the surface. Their results indicated that O-H bond scission is facilitated by the presence of an extra ethanol molecule, while C-H bond dissociation is slightly inhibited by the extra ethanol molecule. Their work highlights the potential solvent effect of ethanol solvent. Accordingly, questions still remain on the nature of solvation effects for ethanol oxidation, which involves C-C and C-H scission, especially using ab initio molecular modeling tools like DFT.

In the current work we addressed solvation effects on the breaking of C-C and C-H bonds, and formation of C-O bond in ethanol oxidation/decomposition over the Rh(111) surface. Rhodium is a promising, important ethanol oxidation catalyst for breaking C–C bonds[18,34,47–53], and has been studied both experimentally and via simulations. Complete oxidation involves several possible intermediates, and the breaking of various bonds (C-C, C-H) in ethanol and reaction intermediates to form CO_2. Reaction and activation energies were calculated using different solvent approaches (implicit, explicit, and hybrid) for bond breaking involving select reaction intermediates involved in ethanol oxidation. These species have been proposed to be critical intermediates for C-C bond breaking of ethanol[18,19,21,54]. C-H bond cleavage was also modeled. C-O bond formation reaction to form acetic acid was also modeled. Acetic acid formation via the oxidation of adsorbed $*CH_3CO$ by *OH species is one of the main side products in ethanol oxidation[45,55–57], and inhibiting C-O bond formation is essential for complete ethanol oxidation. We considered two different solvents, ethanol and water. This approach allows the comparison of different solvent methods and evaluates what role the solvent could have on reaction kinetics. To investigate the effect of the number of explicit solvent molecules, we also modeled explicit solvation with more than one water molecule interacting with the adsorbates and metal surface. Moreover, besides the implicit and explicit solvation models, we applied the bond-additivity model[58,59] to predict heats of adsorption in solvated environments. The bond-additivity method can in principle give heats of adsorption closer to experiment by better describing the energetics of the solvent environment.

2 Methodology

2.1 Computational Details

We performed all calculations using the Vienna ab initio Simulation Package (VASP)[60–63]. We specifically used the GPU version of the code.[64–66] We used projector augmented wave (PAW) pseudopotentials[67,68] to represent core electrons. The number of valence electrons simulated for each atom was 9 for Rh, 4 for C, 1 for H, and 6 for O. We performed tests on the number of valence electrons for Rh (9 or 15) and the results (Table S1) indicate that 9 electrons was suitable for our modeling of Rh. We used a plane wave basis set with a cut-off energy of 400 eV. The Perdew-Burke-Ernzerhof (PBE) exchange correlation functional[69] was used throughout the study. First order Methfessel-Paxton smearing[70] with a smearing width of 0.1 eV was also used. All calculations were spin polarized. The convergence criteria for the self-consistent-field (SCF) energy calculations and atomic forces were to 10^{-6} eV and 0.01 eV/Å, respec-

tively.

The Rh(111) surface was represented by a (3×3) slab which was four layers thick. The bottom two layers of the slab were fixed. The slab had lattice lengths of 8.15 Å with a 20 Å vacuum separation set in the z direction perpendicular to the surface. This slab is shown in Figure S1. The lattice constant of bulk Rh was calculated to be 3.84 Å, which is in agreement with previous work[18,41,52,71]. For the slab calculations, a Gamma centered k-point grid of 4 × 4 × 1 was chosen to sample reciprocal space. To model gas phase molecules, a 20 Å × 20 Å × 20 Å box cell was used. These gas-phase calculations used a Monkhorst Pack k-point grid of 1 × 1 × 1.

We modeled adsorption of several species, and further details on determining stable geometries are discussed in the Supporting Information. A comparison of our vacuum electronic adsorption and reaction energies with literature values indicates the validity of our method (see Tables S2 and S3). We calculated free energies of adsorption when using the various solvation approaches. The Gibbs free energies were calculated using ideal-gas statistical mechanics for gas phase molecules and the harmonic limit approximation for adsorbed species, similar to previous work[46,59,72,73]. Details of how we calculated free energies can be found in the Supporting Information.

In vacuum or with implicit solvation, the adsorption Gibbs free energies involving gas-phase species (e.g. $A+* \longrightarrow *A$, where $*$ refers to the bare metal surface) were determined according to the following formula:

$$\Delta G_{ads}(*A) = G(*A) - G(*) - G(A(gas)). \quad (1)$$

Here $G(*A)$ is the free energy of the adsorbate-surface system, $G(*)$ is the free energy of the bare surface, and $G(A(gas))$ is the free energy of the gas-phase adsorbate molecule. Using explicit solvation, the adsorption free energies of the species were calculated as follows[32,33]:

$$\Delta G^{sol}_{ads}(*A) = G(*(A+solv)) - G(*solv) - G(A(gas)). \quad (2)$$

G(*(A+solv)) is the free energy of the adsorbate/surface with nearby solvent molecule, and G(*solv) is the free energy of the surface with a solvent molecule on the surface. G(*solv) was calculated from the most stable configuration of a solvent molecule (either water or ethanol) on the surface.

In the Supporting Information we discuss how we attempted several different initial configurations with the solvent molecule bound to the surface. For explicit solvation the water solvent molecule was adsorbed at atop site of the surface, while the ethanol solvent molecule was also adsorbed at the atop site. As for explicit+ solvation (discussed below, having two solvent molecules), the most stable structure of the solvent from the explicit method was chosen as the starting point and the second solvent molecule was added to interact with the first solvent molecule in different initial geometries. With two water solvent molecules, the O atom of the second water molecule was bound to the H atom in the first water solvent molecule, as indicated in Figure S7. For the hybrid method, implicit solvation was applied to the most stable structure from the explicit method. To study the effect of solvation on adsorption free energy, we calculated the "adsorption solvation free energy" ($\Delta\Delta G^{sol}_{ads}$), as discussed by Iyemperumal and Deskins[30], and other previous work[32,74–76]. The adsorption solvation free energy represents the energy difference in the adsorption free energies between vacuum and solvated systems:

$$\Delta\Delta G^{sol}_{ads} = \Delta G^{sol}_{ads} - \Delta G^{vac}_{ads}. \quad (3)$$

We modeled C-C bond breaking reactions over the Rh surface for CH_3CH_2OH, CH_3CH_2O, CH_2CH_2O, CH_3CO, CH_2CO, and CHCO. (e.g., $*CH_xCO \longrightarrow *CH_x + *CO$). These reactions have been reported to be the key reaction pathways for C-C bond breaking in ethanol[18,19,21,42,44,54]. For comparison we also modeled C-H bond-breaking (e.g., $*CH_xCO \longrightarrow *CH_{x-1}CO + *H$) and C-O bond formation ($*CH_3CO + *OH \longrightarrow *CH_3COOH$). To calculate the reaction free energies for C-C and C-H bond scission reactions (e.g. $*AB \longrightarrow *A + *B$)) in vacuum and implicit solvation, we used this formula:

$$\Delta G_{rxn} = G(*A) + G(*B) - G(*AB) - G(*). \quad (4)$$

Here $G(*A)$ and $G(*B)$ are the free energies of species A and species B adsorbed on the surface. $G(*AB)$ is the free energy of species AB adsorbed on the surface, and $G(*)$ is the free energy of the clean surface. As for explicit solvation, the reaction free energies were calculated as follows[33,77]:

$$\Delta G^{sol}_{rxn} = G(*(A+solv)) + G(*(B+solv)) \quad (5)$$
$$-G(*(AB+solv)) - G(*solv).$$

To calculate the reaction free energies for C-O bond formation reaction (e.g. $*A + *B \longrightarrow *AB$) in vacuum and implicit solvation, we used this formula:

$$\Delta G_{rxn} = G(*AB) + G(*) - G(*A) - G(*B). \quad (6)$$

As for explicit solvation, the reaction free energies were calculated as:

$$\Delta G^{sol}_{rxn} = G(*(AB+solv)) + G(*solv) \quad (7)$$
$$-G(*(A+solv)) - G(*(B+solv)).$$

Activation energies were calculated using the Brønsted–Evans–Polanyi (BEP) correlations[78–80], which relate the activation energy of an elementary reaction step to the corresponding reaction energy of that step. The accuracy and utility of these correlations have been demonstrated in previous work[19,81–83]. Ferrin et al. developed BEP correlations for C-C and C-O scission in ethanol decomposition on ten transition metal surfaces[19]. Wang et al.[81,82] developed a linear scaling relationship between dissociation energies and transition state energies for C–C, C–O, C–N, N–O, N–N, O–O dissociation reactions and (de)hydrogenation reactions over transition metals. Sutton et al.[83] also developed a BEP correlation for C-H, O-H, C-C, and C-O bond-breaking on Pt(111) surfaces. Scaling relationships have been utilized not only for metal surfaces in vacuum, but

have also been demonstrated to be applicable for implicit, explicit, and hybrid solvation models[20,84,85]. Regarding explicit solvation, Zaffran et al.[84] showed that BEP parameters for C-H scission were very similar in vacuum and explicit environments. In addition, Gomes et al.[86] developed a BEP relationship with implicit solvation for water dissociation reactions. They showed that activation energy barriers are only slightly influenced by the inclusion of the implicit solvent. As discussed in the Supporting Information, we utilized the parameters of Wang et al.[81,82] in this work. This consistency in the BEP model (as opposed to using different BEP models with different solvation environments) allows us to directly assess the solvation approaches without having to worry that any variations may be due to using different BEP parameters. The BEP correlations were fitted to electronic energies, rather than Gibbs free energies. Hence, for results involving activation energies we utilized energies, rather than free energies. The exception to this occurred when we used implicit solvation, as discussed in the Supporting Information, where more details on the activation energy calculations can be found.

2.2 Solvation Models

Explicit solvation approaches add solvent molecules directly to the simulation, while implicit solvation approaches use a continuum to represent the solvent. We considered both approaches in this work, as well as a hybrid solvation approach. For explicit solvation, we added extra solvent molecules (e.g., water or ethanol) to the slab-adsorbate system. We considered one solvent molecule (labeled the explicit method) or two solvent molecules (labeled the explicit+ method). To quantify solvation effects, we compared the adsorption free energies of each intermediate and the reaction free energies of C-C and C-H bond breaking in vacuum, explicit solvent, implicit solvent, and hybrid solvent environments. For implicit solvation modeling, we used the VASPsol code[26]. We used dielectric constants of 78.4 for water and 25.02 for ethanol, which are appropriate values near room temperature.[87,88] As for hybrid models, explicit solvent molecules were added to the simulation while implicit solvation was also applied. Figure S2 shows ethanol adsorbed in these various solvent environments. Details on how we determined surface geometries using these different solvation models are further discussed in the Supporting Information. In this work we calculated vibrational, rotational, and translational contributions to free energy, as discussed in the Supporting Information. The implicit free energy also includes configurational entropy of the solvent molecules, which is not present in our explicit calculations. It is possible to obtain solvation configurational entropy with explicit solvation, for instance by performing molecular dynamics simulations[32,36,89], but such calculations are beyond the scope of the current work. Our explicit calculations do not include this configurational solvation energy term, while the implicit solvation calculations do include the configurational entropy of the solvent. However, the implicit solvation energies are small (an average of -0.06 eV in water and -0.02 eV in ethanol), as Figure S9 shows. Accordingly, the configurational entropy of the solvent molecules present in implicit solvation is small. Therefore, even though we neglect configurational entropy in our explicit solvation calculations, we are still able to compare the various solvation method free energies. Other researchers[85] have had a similar approach to compare implicit and explicit solvation results.

2.3 Bond-Additivity Model

Besides implicit and explicit solvation methods, the bond-additivity approach also can be used to estimate the adsorption enthalpy at metal-aqueous interfaces. This approach was used by Singh and Campbell[58] to analyze the heat of adsorption of phenol over Pt(111) in aqueous phase. Akinola et al.[59] then utilized the bond-additivity approach with DFT calculations to predict the adsorption enthalpies of several organic species over Pt(111) and Rh(111) in aqueous phase. They showed that implicit solvation calculations overpredicted adsorption enthalpies compared with experimental measurements, while the bond-additivity model had much closer agreement with experimental values. Therefore, the bond-additivity approach is a promising method to predict the adsorption enthalpy at metal-aqueous interfaces. Further details on how we implemented the bond-additivity approach are found in the Supporting Information.

3 Results and Discussion

We calculated adsorption free energies of several adsorbates in vacuum and various solvation environments. These solvation models were used: implicit, explicit, and hybrid solvation models. Reaction free energies (ΔG_{rxn}) and activation energies (E_a) for C-C and C-H bond breaking, and C-O bond formation were also computed to compare in vacuum and solvents. Both water and ethanol were studied as solvents. Finally, the bond-additivity solvation approach was also applied to calculate the adsorption enthalpies in water.

3.1 Effect of Water Solvation on Ethanol Oxidation

We applied implicit, explicit, and hybrid solvation models to the modeling of adsorption and ethanol oxidation reaction steps in water solvent. Calculated adsorption free energies are given in Table S22. Adsorption solvation free energies represent the energy differences for adsorption between vacuum and liquid phases, and are shown in Figure 1. Figures 2 (C-C bond breaking) and 3 (C-H bond breaking and C-O bond formation) present reaction free energies and activation energies for various reactions.

We first examine our results using implicit water solvation, which show that the implicit solvation model had only a small effect calculated energies. As shown in Figure 1, the adsorption solvation free energies using implicit solvation were small, and ranged from -0.07 to 0.13 eV, with an average change of 0.03 eV when compared to the vacuum phase. The adsorption solvation energies for some of these species (CH_3CH_2OH, CH_3CO, CH_2CO, CHCO, CH_3, CH_2, CH, CO, H) were reported to be in the range of -0.04 to 0.10 eV in Iyemperumal et al.'s work[30], similar to the current work. For reactions involving C-C scission (Figure 2), the reaction free energies and activation energies changed with an average value of -0.05 eV relative to the vacuum, and the largest

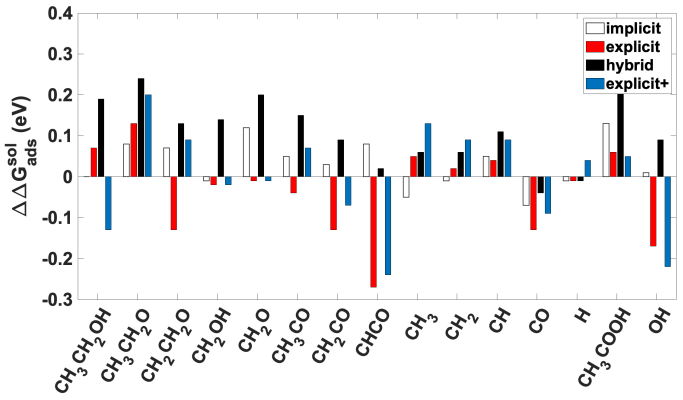

Fig. 1 Adsorption solvation free energies on Rh(111) of several species relevant to ethanol oxidation. Water was the solvent for these calculations. Some adsorption solvation values are very small, and do not appear as actual bars because of this (e.g. OH with hybrid solvation).

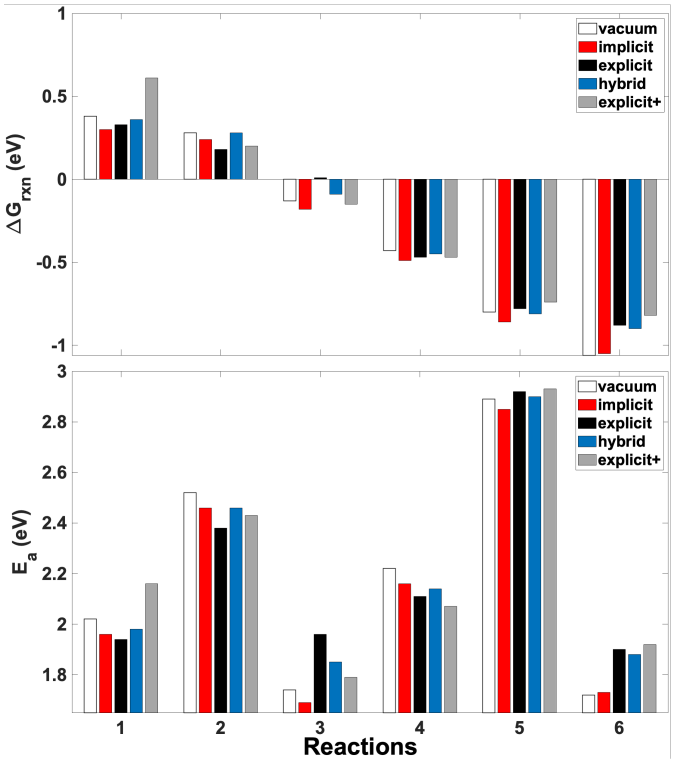

Fig. 2 Reaction free energies and activation energies for C-C bond breaking in water over Rh(111) using various solvation models. Indicated are reaction free energies and activation energies. Reactions involved: (1) $CH_3CH_2OH \rightarrow CH_3 + CH_2OH$; (2) $CH_3CH_2O \rightarrow CH_3 + CH_2O$; (3) $CH_2CH_2O \rightarrow CH_2 + CH_2O$; (4) $CH_3CO \rightarrow CH_3 + CO$; (5) $CH_2CO \rightarrow CH_2 + CO$; (6) $CHCO \rightarrow CH + CO$.

energy change was -0.08 eV. These results agree with previous work reported in the literature[20], were it was reported that reaction energies became more exothermic using implicit water solvation by -0.02 eV on average for the same select C-C bond scissions that we modeled. For C-H bond scission, again reaction free energies with implicit solvation only changed slightly compared to vacuum (Figure 3). As for C-O bond formation, reaction free energy changes were larger than C-H bond breaking with implicit water solvation and increased by 0.08 eV compared to vacuum. The activation energy was barely affected by implicit water solvation and only increased by 0.01 eV. Finally, analysis indicates that implicit solvation changed adsorbate geometries little when compared to vacuum, as discussed further in the Supporting Information, where we show the optimized geometries and provide bond distances between atoms.

When using the explicit model with only one water molecule, the adsorption of several species were stabilized compared to the vacuum calculations. The average adsorption free energy change was -0.03 eV compared to vacuum, with the largest energy change being -0.27 eV for the adsorption of CHCO. Hydrogen bonds formed between the adsorbates and explicit water molecules, as the various Figures S10 to S24 show. The distances between adsorbates and the metal surface changed with an average value of 0.03Å, while the minimal and maximum surface-adsorbate distances changes were 0.00 and 0.18 Å. Upon hydrogen bond formation, the water molecules interacted with the adsorbates strongly (average H-bond distance of 1.73 Å) or weakly (average H-bond distance of 2.57 Å). Those adsorbates which were not stabilized by explicit solvation did not form hydrogen bonds with the water solvent molecule. Favorable intermolecular hydrogen bonding can lead to stronger adsorption of surface species, as indicated in literature[32–34,53,90] and our current work. This hydrogen bonding is not described by implicit solvation. Explicit solvation also affected reaction free energies and activation energies for C-C scission, as Figure 2 shows. The average reaction and activation energy change relative to the vacuum was only 0.03 and 0.02 eV, but for key species like CH_xCO, the energy changes could be consequential. The activation energy of CH_3CO decreased by 0.10 eV, while the activation energies of CH_2CO and CHCO increased by 0.03 and 0.18 eV, respectively. An activation energy decrease of 0.1 eV at 298 K could increase the rate constant by ~50, assuming an Arrhenius expression and constant pre-exponential factors ($\frac{k_2}{k_1} = exp(\frac{E_{a1}-E_{a2}}{RT})$). Therefore, the activation energy decrease using explicit water solvent could significantly promote the reaction rate. Explicit water solvation also had an important impact on C-H scission, with the average reaction free energy and activation energy change being -0.13 and -0.16 eV. C-O bond formation reaction was inhibited using explicit water solvation with the reaction free energy and activation energies increased by 0.27 eV and 0.41 eV. This increase will most certainly inhibit acetic acid formation.

When applying explicit+ solvation with two water solvent molecules, adsorption free energies changed in the range of -0.24 to 0.20 eV compared to vacuum adsorption free energies. For some species (CH_3CH_2O, CH_3, CH_2, and CH) that were not stabilized, only weak hydrogen bonds formed between adsorbate and water solvent for CH_2, as indicated by very long (~2.5 Å) hydrogen-adsorbent bond lengths; while no adsorbate-water H-bonding formed for CH_3CH_2O, CH_3, and CH species, which all had adsorption free energy increases between only 0.03 to 0.14 eV. Species with significant hydrogen bond formation were stabilized on the surface to a greater extent. For C-C cleavage, reaction free energy and activation energy changes ranged from -0.08 to

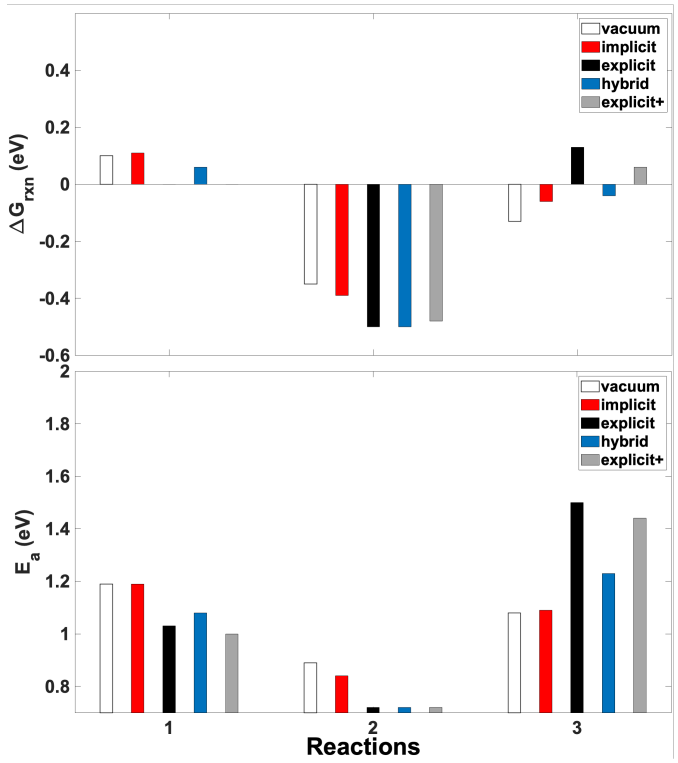

Fig. 3 Reaction free energies and activation energies for C-H bond breaking and C-O bond formation in water over Rh(111) using various solvation models. Indicated are reaction free energies and activation energies. Reactions involved: (1) $CH_3CO \rightarrow CH_2CO + H$; (2) $CH_2CO \rightarrow CHCO + H$; (3) $CH_3CO + OH \rightarrow CH_3COOH$.

0.24 eV and from -0.15 to 0.19 eV, which as discussed above could lead to significant changes in rate constants and rates. For example, for scission of CHCO, the reaction free energy increased by as large as 0.24 eV. Some energy changes were small, for example, the reaction free energies of CH_2CO only increased by 0.07 eV. As for C-H cleavage, the average reaction free energy and activation energy changes were -0.12 and -0.18 eV, again indicating that explicit+ solvation could have a notable affect on C-H scission. The reaction free energies and activation energies of C-O bond formation increased by 0.19 and 0.36 eV using the explicit+ method (similar to explicit solvation), which would inhibit acetic acid formation and promote full oxidation.

Adsorption solvation free energies, as shown in Figure 1, varied between -0.04 to 0.33 eV when using the hybrid model. The average adsorption free energy change relative to vacuum was 0.12 eV. As a combination of the implicit and explicit method, the hybrid method's adsorption free energies were more endothermic than both the implicit and explicit method for most of the adsorbates. The hybrid approach had minimal effect on adsorbates' structures (bond lengths changed within 0.03 Å), while the distances between the adsorbates and metal surfaces were affected slightly more (distances changed up to 0.18 Å), all discussed further in the Supporting Information. Hydrogen bonding formed between explicit water molecules and adsorbates (except for CH_3, CH, and H). As shown in Figure 2, the largest reaction free energy change was 0.16 eV for the C-C bond scission of CHCO, while the smallest change occurred with CH_2CO by 0.00 eV. For C-H, as indicated in Figure 3, both of the CH_3CO and CH_2CO bond breaking reaction free energies decreased, and the average reaction free energy and activation energy change were -0.10 and -0.14 eV for C-H reactions. Overall, the hybrid method had an important impact on energies, similar to the explicit and explicit+ solvation methods. As for C-O formation, the reaction free energy increased by 0.10 eV and the activation energy also increased by 0.15 eV, indicating that hybrid water solvation hindered formation of acetic acid.

3.2 Comparing Water Solvation Methods in Water

Figure 4 shows a summary comparing the various solvation methods, giving the calculated adsorption and reaction free energies relative to vacuum. Upon applying a solvent, activation energy changes were very similar to reaction free energy changes due to the linear relationship between reaction and activation energies. As indicated and already discussed, implicit solvation had small affect on adsorption, reaction, and activation energies. There was quite a spread in adsorption free energy changes when applying explicit, explicit+, and hybrid solvation methods. The largest energy decrease in water for the adsorption free energies was -0.27 eV when using the explicit method, while the largest energy increase was 0.33 eV using hybrid method. The largest range of adsorption free energy changes (-0.24 to 0.20 eV) occurred when using the explicit+ solvation method.

As for reaction free energies and activation energies, the explicit, explicit+, and hybrid approaches led to both significant positive and negative energy changes. Of these three methods, the hybrid method had the smallest impact on breaking C-C bonds (maximum and minimum changes of -0.02 and 0.16 eV). The largest energy decrease for the C-C bond scission reaction free energies energies was -0.10 eV when using the explicit method, while the largest energy increase was 0.24 eV using explicit+ method. Explicit method had the largest impact on C-H scission of both CH_3CO and CH_2CO with the reaction free energies decreased by -0.10 and -0.15 eV. As for C-O bond formation, explicit water solvation had the largest impact, as the reaction free energies and activation energies increased by 0.27 and 0.41 eV. Overall, the explicit+ method had the largest effect on C-C bond scission with the reaction free energy changes ranging from -0.08 to 0.24 eV, while explicit method had the largest impact on breaking C-H bond and forming C-O bond. We notice that applying implicit solvation to vacuum had a smaller effect than applying implicit to explicit (hybrid) solvation, as the differences between explicit and hybrid results are more profound (Figure 4). When implicit solvation is applied to vacuum calculations only the adsorbate and surface interact with the solvent continuum. On the other hand when implicit solvation is applied to explicit structures, then the surface, adsorbate, and solvent molecule all interact with the solvent continuum. Thus larger interactions may occur when an explicit solvent molecule is present, and hence the greater effect of implicit solvation on explicit structures.

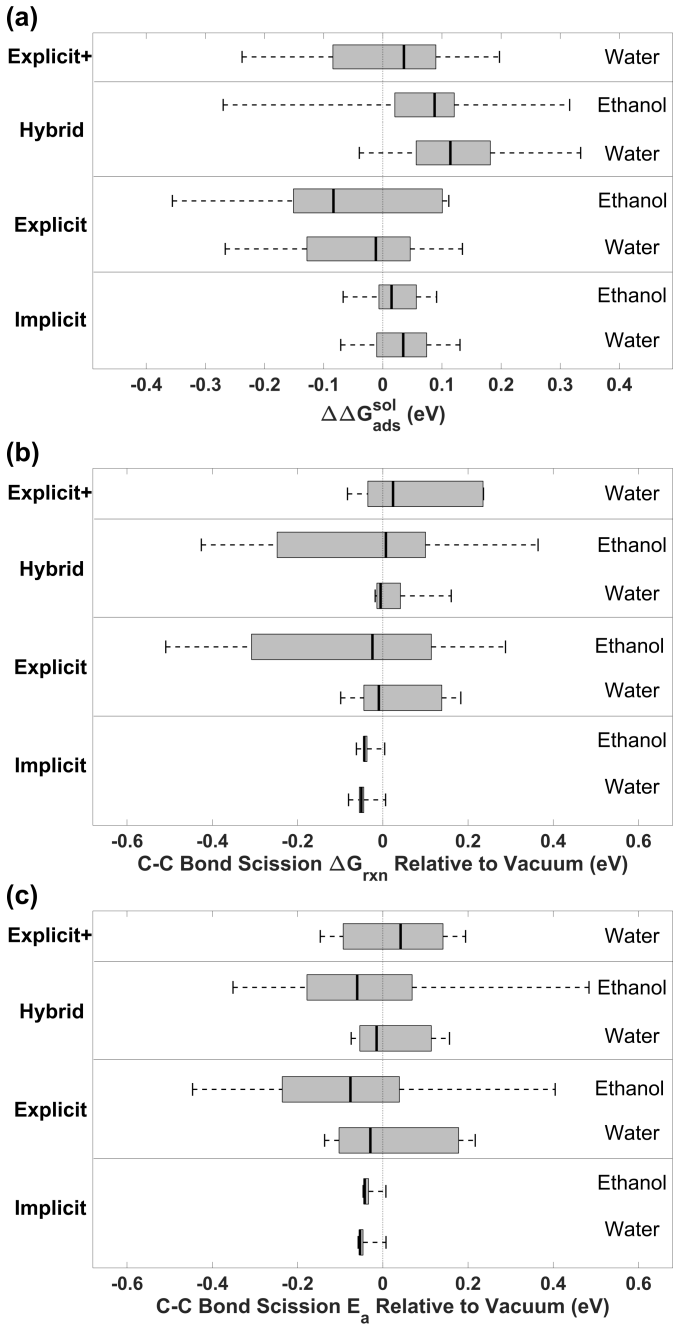

Fig. 4 Box plots summarizing changes in (a) adsorption free energies, (b) reaction free energies, and (c) activation energies for C-C bond scission in water and ethanol liquid environments.

We must add one caveat regarding the effect of solvation. The median energy changes (as shown in Figure 4) were all small (less than $\sim$ 0.1 eV). Indeed changes for some reaction free energies when applying solvation were small, as Figure 2 shows, e.g. C-C scission of CH_2CO. Thus, solvation does not always lead to large energy changes, and such changes are dependent on the chemical species. Our conclusions regarding C-C scission agree with work out of the Heyden group[36]. They showed that in implicit and explicit (eSMS) water environments, reaction free energies for C-C scission of ethylene glycol only increased by 0.11 and 0.10 eV, and activation free energies increased by 0.11 and 0.21 eV, respectively. They have also shown[23] that C-H bond scission of ethylene glycol can be slightly promoted when using explicit (eSMS) water solvation, where the reaction free energy changed by -0.02±0.06 eV and activation free energy changed by -0.16±0.05 eV. Changes in reaction energies may not always be large under solvation.

3.3 Ethanol Oxidation in Ethanol Solvent

So far we have reported results where water was the solvent. We next examine how different solvation methods treat another solvent, namely ethanol. These calculations were motivated by recent work which showed room-temperature oxidation to occur in ethanol solvent[25]. The adsorption free energies when using ethanol solvent are given in Table S39, while adsorption solvation free energies are given in Figure 5. The reaction free energies are shown in Figures 6 and 7.

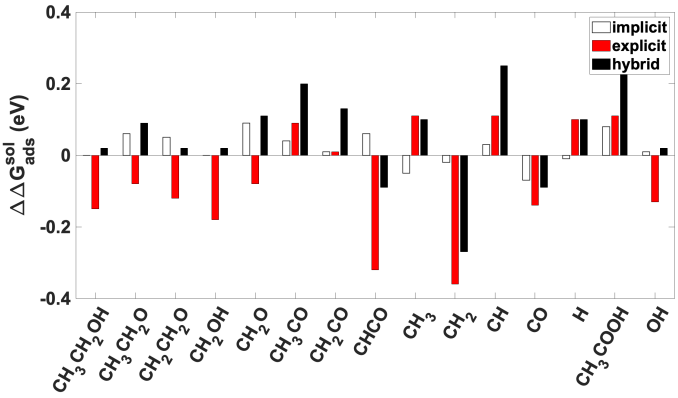

Fig. 5 Adsorption solvation free energies on Rh(111) of several species relevant to ethanol oxidation. Ethanol was the solvent for these calculations. Some implicit adsorption solvation values are very small, and do not appear as actual bars because of this.

Similar to our results in water solvent, implicit solvation had only a small impact on energies, while explicit and hybrid solvation changes energies significantly. Figure 5 indicates that changes in adsorption free energies using implicit solvation were small. Figures 6 and 7 also indicate that the implicit approach had minimal effect on the reaction free energies compared to vacuum. When we applied explicit solvation the adsorption free energies changed significantly. The average adsorption free energy change was -0.07 eV, and the largest change was -0.36 eV for CH_2. C-C scission reaction free energies also changed considerably when applying explicit solvation, with changes ranging from -0.51 to 0.29 eV. C-H scission reactions changed by 0.03 (CH_3CO) and -0.23 (CH_2CO) eV when applying explicit solvation, while C-O bond formation reaction free energies increased by 0.15 eV. Hybrid solvation also had several large changes in adsorption free energy, with the largest energy decrease being -0.27 eV for CH_2 and the largest adsorption free energy increase being 0.32 eV for CH_3COOH. C-C scission reaction free energies changes ranged from -0.43 to 0.36 eV with hybrid solvation, while C-H scission reaction free energies changes were 0.06 (CH_3CO) and -0.20 (CH_2CO) eV. As for C-O bond formation, reaction free energy and activation energies both increased by 0.11 eV when

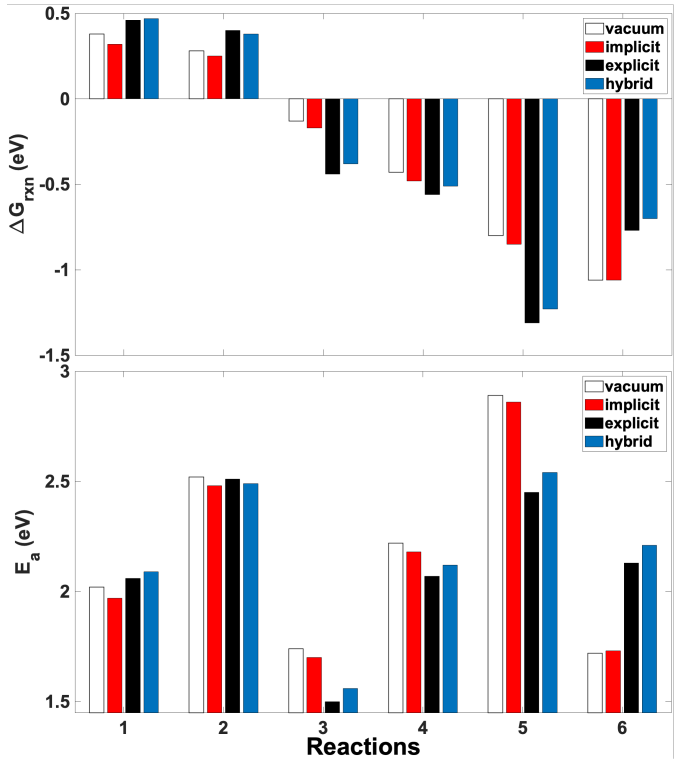

Fig. 6 Reaction free energies and activation energies for C-C bond breaking in ethanol solvent using various solvation models. Indicated are reaction free energies and activation energies. Reactions involved: (1) $CH_3CH_2OH \rightarrow CH_3 + CH_2OH$; (2) $CH_3CH_2O \rightarrow CH_3 + CH_2O$; (3) $CH_2CH_2O \rightarrow CH_2 + CH_2O$; (4) $CH_3CO \rightarrow CH_3 + CO$; (5) $CH_2CO \rightarrow CH_2 + CO$; (6) $CHCO \rightarrow CH + CO$.

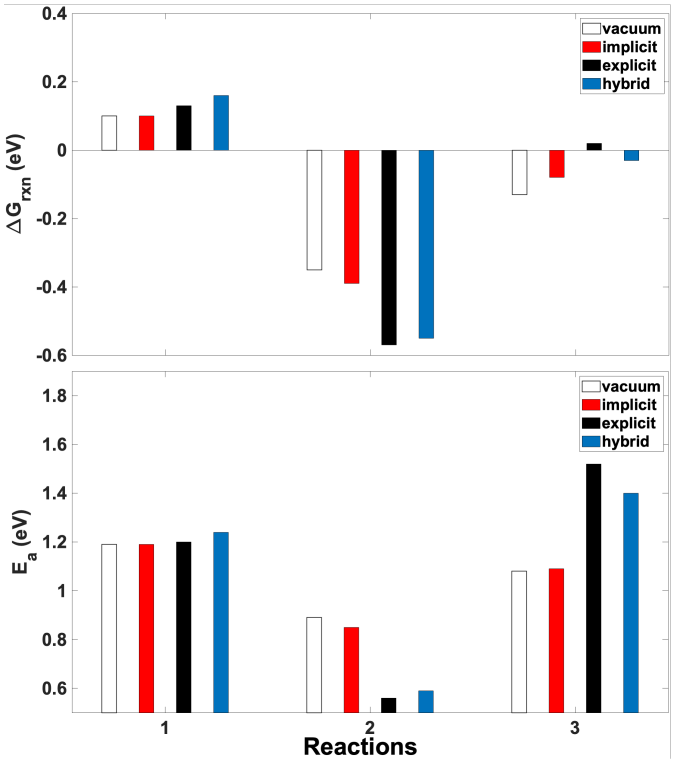

Fig. 7 Reaction free energies and activation energies for C-H bond breaking and C-O bond formation in ethanol solvent using various solvation models. Indicated are reaction free energies and activation energies. Reactions involved: (1) $CH_3CO \rightarrow CH_2CO + H$; (2) $CH_2CO \rightarrow CHCO + H$; (3) $CH_3CO + OH \rightarrow CH_3COOH$.

using hybrid ethanol solvation. Figure 4 presents a summary and comparison of the different solvation method results with ethanol solvent. Again, as shown, implicit solvation had little affect on adsorption and reaction free energies, while explicit and hybrid solvation significantly changed these energies for several species.

3.4 Comparing Water and Ethanol Solvents

Water is one of the most commonly used liquid in catalysis, while other liquids may also be used for solvation. We have already mentioned the effectiveness of ethanol solvent.[25] As reported by Fortunelli et al.[91,92], tuning the dielectric constant of the solvent can result in a faster oxygen reduction reaction. Heyden's group[93] also studied the effect of solvent choice for hydrodeoxygenation processes over Pd, and found that solvent choice could affect catalytic activity. In the current work, different solvents (water and ethanol) were studied to simulate the liquid-metal interface for select C-C and C-H bond scission as well as C-O bond formation. Figure 4 compares calculated energies in both water and ethanol environments. Using the implicit solvation method, water and ethanol had a similar solvation effect on the adsorption free energies, which was small. Reaction free energy changes were also small using implicit solvation in water and ethanol solvents.

With explicit solvation, ethanol solvent overall had a larger impact on calculated energies. As shown, explicit solvation with ethanol solvent had a slightly larger range of adsorption free energy changes compared to water solvent. The range in reaction free energy changes for C-C scission was significantly larger in ethanol solvent compared to water solvent (-0.51 to 0.29 eV for ethanol and -0.10 to 0.18 for water). Hybrid solvation exhibited similar results, where ethanol solvent had a larger impact than water solvent on free energies. Our results help explain why ethanol has been observed to be an effective solvent for ethanol oxidation[25], because of the significant energy changes in ethanol solvent. Our work also highlights the importance of assessing different solvents to control catalytic performance.

3.5 Effect of Solvation on C-C Scission

While ethanol oxidation may involve many different reactions, C-C scission is the bottleneck for efficient complete oxidation of ethanol. Previous research involving vacuum phase calculations[18,21] has shown that breaking of CHCO had the lowest activation energy of various $CH_xCH_yOH_z$ reaction intermediates, and is the preferred reaction pathway for complete ethanol oxidation over the Rh(111) surface in vacuum. As we have shown, both water and ethanol solvents can have considerable impact on ethanol oxidation/decomposition, illustrating the importance of solvent choice and model. Indeed, it has been shown[94] that methanol electro-oxidation has different reactivity when using a hybrid solvation model compared to vacuum. To further investigate the impact of solvation on reactions, we compared the activation en-

ergies of C-C scission reactions in both liquid water and ethanol. Figures 2 and 6 provide the activation energies, while Figure 8 ranks the various C-C breaking reactions according to activation energy to identify preferred reaction pathways.

Fig. 8 Ranking of activation energies for C-C scission of different reactants using different solvation approaches. Numbers are activation energies for C-C scission in eV for the given reactant. Results are shown in (a) water solvent and (b) ethanol solvent.

In the vacuum phase, C-C bond breaking of CHCO had the lowest activation energy (1.72 eV) among the modeled reactants. Thus, the preferred pathway for C-C scission in vacuum should involve CHCO instead of other reactants. This agrees with previous literature[18,21]. However we do note that CH_2CH_2O had a very similar activation energy in vacuum (1.74 eV), so scission of this species is likely competitive with CHCO. Figure 8 shows that in water solvation, C-C scission via CHCO was still the most preferred reaction pathway with the explicit solvation method. However, the most favorable reaction pathway involved CH_2CH_2O when using the implicit, hybrid, and explicit+ methods, with CHCO being the second most favorable reactant. However, for a chosen solvation approach the activation energies of the first and second most favorable reactants were very similar (0.02 to 0.13 eV difference). Thus the first and second most favorable reactants will compete for C-C scission, irregardless of solvation approach. Even the third most favorable reactants had similar activation activation energies compared to the most favorable reactant, only being more endothermic by 0.06 to 0.30 eV depending on the solvation method. Thus, in water solvent the preferred pathway depends on the solvation approach, but several competing pathways may occur.

As for ethanol solvation, Figure 8 shows that the preferred reactant for C-C scission can change dramatically depending on the solvation method with ethanol solvent. For example, scission of CH_2CH_2O was easiest using all solvation methods with ethanol, and scission of CHCO became much harder using explicit and hybrid solvation methods. This is in contrast to water solvent, where CHCO had among the lowest activation energies. Also unlike water solvent, in ethanol solvent using explicit and hybrid solvation methods a clear distinction occurs (i.e. no close activation energies) so that competition between reactants diminishes. For example, with explicit solvation CH_2CH_2O had the lowest C-C scission activation energy, while CH_3CH_2OH (the second most favorable reactant) had an activation energy 0.56 eV higher. Similar behavior occurs with hybrid solvation. Thus, with ethanol solvent when explicit molecules are added, the most favorable pathway for C-C scission becomes readily apparent, unlike with water solvent where several reactants have similar activation energies.

Our results show that the preferred reaction pathway for C-C scission depends on the solvation environment, such as choice of solvent (water or ethanol) and solvation model. Indeed, the preferred reactant for C-C scission changes drastically depending on the solvent. In vacuum a 'late' reactant that has undergone many dehydrogenation steps (CHCO) has the lowest activation energy for C-C scission. However, in ethanol solvent (all solvation models) and water solvent (implicit, hybrid, explicit+ solvation models) an 'early' reactant involving only two dehydrogenation steps (CH_2CH_2O) had the lowest activation energy. This has strong implications on the ethanol oxidation reaction, as C-C scission of an 'early' reactant involves fewer activated steps and could increase the efficiency of complete oxidation. We note that several reactants are competitive for C-C scission in water due to close activation energies (CHCO, CH_2CH_2O). The situation changes in ethanol solvent. When using implicit solvation, CHCO and CH_2CH_2O have close C-C scission activation barriers. However, CH_2CH_2O is distinctly preferred (lowest activation barrier by $\sim$ 0.5 eV) when using explicit and hybrid solvation approaches. Given these results, it would seem that a favored C-C scission pathway is more clearly evident in ethanol solvent when using more robust solvation methods.

3.6 Bond-Additivity Model

The bond-additivity model was used to predict heats of adsorption over Rh(111) surfaces by adding in corrections to DFT-calculated enthalpies. As discussed in the Supporting Information, calculating enthalpies involves more in-depth calculations, such as vibrational frequencies. As such, calculating enthalpies using DFT is not 'routine' in the literature. Nevertheless, having enthalpies can prove valuable for better understanding surface processes. In this work, we calculated adsorption enthalpies for intermediates in C-C and C-H bond scission reactions. The calculated adsorption enthalpies in vacuum and liquid water phases are listed in Table 1. The bond-additivity enthalpies were $\sim$ 1.1 eV on average more endothermic than the enthalpies from the other solvation approaches. The smallest adsorption enthalpy increase was 0.64 eV for CH (compared to implicit water solvation), while

the largest enthalpy increase was 1.51 eV for CHCO (compared to explicit+ water solvation). Therefore, when using the bond-additivity method, adsorption became weaker on the metal surface for all adsorbates. However, as shown in Figure 9, the trends in adsorption enthalpies are consistent when using the various solvation approaches. For instance, CH_3CH_2OH had the highest adsorption enthalpy and CH had the lowest adsorption enthalpy for all methods. Figure 9 indicates that while absolute adsorption energies differ for each solvation approach, the relative ordering of adsorption energies for the various species are similar for the different solvation methods.

Table 1 Calculated adsorption enthalpies of species relevant to ethanol oxidation. Results are in water solvent.

	ΔH_{ads} (eV)					
	vacuum	implicit	explicit	hybrid	explicit+	bond-additivity
$*CH_3CH_2OH$	-0.36	-0.37	-0.40	-0.28	-0.61	0.62
$*CH_3CH_2O$	-2.21	-2.13	-2.15	-2.05	-2.19	-1.24
$*CH_2CH_2O$	-1.23	-1.16	-1.55	-1.29	-1.40	-0.21
$*CH_2OH$	-2.05	-2.06	-2.21	-2.06	-2.24	-1.20
$*CH_2O$	-0.86	-0.74	-0.99	-0.78	-1.06	0.17
$*CH_3CO$	-2.37	-2.32	-2.55	-2.36	-2.50	-1.36
$*CH_2CO$	-1.41	-1.38	-1.73	-1.51	-1.72	-0.35
*CHCO	-3.40	-3.41	-3.87	-3.67	-3.90	-2.38
$*CH_3$	-1.84	-1.89	-1.81	-1.80	-1.79	-0.75
$*CH_2$	-4.12	-4.13	-4.18	-4.15	-4.16	-3.13
*CH	-6.69	-6.64	-6.75	-6.68	-6.74	-5.99
*CO	-1.93	-2.00	-2.26	-2.17	-2.25	-0.83
*H	-2.56	-2.58	-2.76	-2.77	-2.73	-1.47

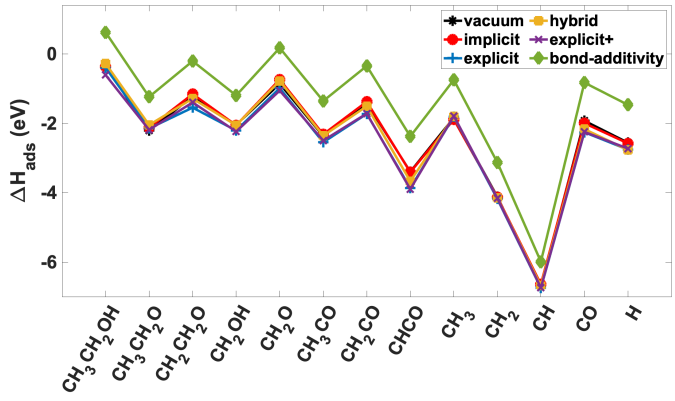

Fig. 9 Adsorption adsorption enthalpies on Rh(111) of several species relevant to ethanol oxidation. Water was the solvent for these calculations

To assess the effect of the bond-additivity approach and its corrections on reactions, we estimated the changes in the heats of reaction from the adsorption enthalpy changes. For surface bond breaking reactions like $AB* \longrightarrow A* + B*$, the heat of reaction can be calculated as $\Delta H_{rxn-surf} = H(A*) + H(B*) - H(AB*) - H(*)$. The heat of reaction can also be broken into contributing components:

$$\Delta H_{rxn-surf} = \Delta\Delta H_{ads} + \Delta H_{rxn-free-species}. \quad (8)$$

$$\Delta\Delta H_{ads} = \Delta H_{ads}(*A) + \Delta H_{ads}(*B) - \Delta H_{ads}(*AB). \quad (9)$$

$$\Delta H_{ads}(*X) = H(*X) - H(*) - H(X_{free}) \quad (10)$$

$$\Delta H_{rxn-free-species} = H(A_{free}) + H(B_{free}) - H(AB_{free}). \quad (11)$$

$\Delta H_{ads}(*X)$ is the adsorption enthalpy of species X (A, B or AB). $\Delta H_{rxn-free-species}$ is the reaction heat of the isolated molecules, while $H(A_{free})$, $H(B_{free})$, and $H(AB_{free})$ are the enthalpies of the free molecules. For the the vacuum, explicit and explicit+ solvation methods, the enthalpies of free molecules were just gas-phase values. For the implicit and hybrid solvation methods, the enthalpies of free molecules were calculated from lone molecules under implicit solvation. We used gas-phase calculations to obtain $\Delta H_{rxn-free-species}$ with the bond-additivity method, consistent with how we calculated adsorption enthalpies with the bond-additivity method. We note that we calculated the differences in energies for gas-phase molecules and molecules with implicit solvation to be only 0.10 eV on average (Table S41). We also note that more exact enthalpies of free molecules may be obtained by considering such molecules in a proper solvent (e.g. surrounded by several solvent molecules), but such calculations are time-intensive and do not change the general trends of our reaction analysis. In these equations, $\Delta\Delta H_{ads}$ represents the adsorption enthalpy difference between reactants and products. Thus, the surface reaction enthalpy has two contributions: adsorbate enthalpy difference and the free reaction enthalpy. The main effect of the bond-additivity method is to provide refinement of the heat of adsorption values, or $\Delta\Delta H_{ads}$ in Equation (8).

Figure 10 shows the calculated $\Delta\Delta H_{ads}$ values for C-C scission reactions using the various water solvation methods. $\Delta\Delta H_{ads}$ values for C-C scission using the bond-additivity method were more endothermic by an average of about 1.1 eV compared to the other solvation values. Furthermore, $\Delta\Delta H_{ads}$ values for C-H scission using the bond-additivity method were more endothermic by an average of about 1.3 eV compared to the other solvation values. Accordingly, the $\Delta H_{rxn-surf}$ values of C-C bond scission using the bond-additivity method are also ~1.1 eV more endothermic compared to the other solvation approaches. This reflects the fact that $\Delta\Delta H_{ads}$ values is a component of $\Delta H_{rxn-surf}$, as Equation 8 shows. The bond-additivity approach better considers the water solvent, and should give more realistic adsorption and reaction enthalpies. Such enthalpies are more endothermic than other calculated enthalpies. However, the trends in reactivity are largely the same for all the solvation methods. For instance, the lowest reaction enthalpy occurs for the scission of CHCO using all of the solvation approaches. Thus, trends and details on reaction behavior can be obtained using methods other than the bond-additivity approach, even if the absolute energies from such solvation methods may not fully agree with experimental data like the bond-additivity method does.

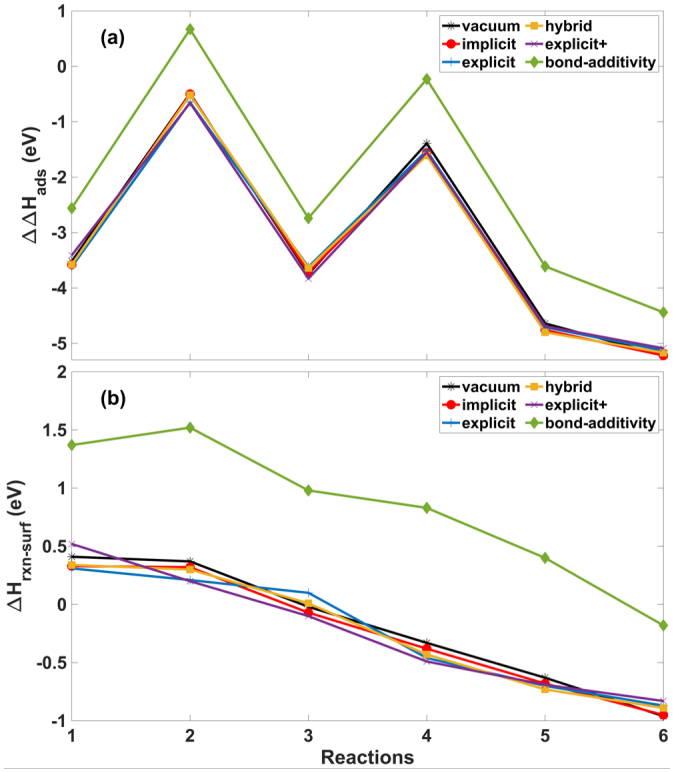

Fig. 10 Calculated (a) $\Delta\Delta H_{ads}$ and (b) $\Delta H_{rxn-surf}$ values for several reactions involving C-C scission. The reactions are as follows: (1) $CH_3CH_2OH \rightarrow CH_3 + CH_2OH$; (2) $CH_3CH_2O \rightarrow CH_3 + CH_2O$; (3) $CH_2CH_2O \rightarrow CH_2 + CH_2O$; (4) $CH_3CO \rightarrow CH_3 + CO$; (5) $CH_2CO \rightarrow CH_2 + CO$; (6) $CHCO \rightarrow CH + CO$.

4 Conclusions

In this study, we addressed how different solvation methods can be used to calculate adsorption free energies and model C-C/C-H bond scission and C-O bond formation over Rh(111), all which may occur during ethanol oxidation/decomposition. The impact of implicit, explicit, and hybrid solvation models with water and ethanol as solvents was investigated. We found that implicit solvation had limited effect on adsorption and reaction free energies. The explicit and hybrid models changed reaction and activation energies (compared to vacuum) for some reactants significantly. These changes were more pronounced with ethanol solvent than with water solvent. We also addressed the effect of the number of solvent molecules with explicit solvation, and found that when using one or two water molecules, the energies were often similar.

In water and ethanol environments, the preferred reaction pathway for C-C scission (the bottleneck of complete ethanol oxidation) depended on the solvation approach. With water solvent, several reactants had similar activation energies, while with ethanol solvent the relative differences in activation energies were larger. We used a bond-additivity model to predict heats of adsorption that should in principle agree better with experimental enthalpies. Using this bond-additivity method we found that predicted heats of adsorption and reaction enthalpies were more endothermic compared to vacuum, implicit, explicit, and hybrid water solvation results. The bond-additivity enthalpies were ∼1.1 eV more endothermic compared to other solvation methods for nearly all the reactants/reactions, and the trends using the different solvation models were consistent with the bond-additivity results. In conclusion, we have evaluated how different solvation models affect the energetics of important steps in ethanol oxidation/decomposition, and we also showed how two different solvents (ethanol and water) can lead to different reactivity. This has strong implications on catalytic reactions when a liquid solvent is present. Our work also emphasizes the need to better understand and model solid-liquid interfaces in order to more accurately predict reaction mechanisms.

Acknowledgements

This work was supported by the National Science Foundation under Grant No. 1511672. We also acknowledge the computational resources provided by Worcester Polytechnic Institute.

Notes and references

1 F. Barbir and T. Gómez, *International Journal of Hydrogen Energy*, 1997, **22**, 1027–1037.
2 X. Li and I. Sabir, *International Journal of Hydrogen Energy*, 2005, **30**, 359–371.
3 A. S. Aricè, P. Cretì, P. L. Antonucci and V. Antonucci, *Electrochemical and Solid-State Letters*, 1998, **1**, 66–68.
4 M. Z. Kamarudin, S. K. Kamarudin, M. S. Masdar and W. R. Daud, *International Journal of Hydrogen Energy*, 2013, **38**, 9438–9453.
5 K. S. Roelofs, T. Hirth and T. Schiestel, *Materials Science and Engineering: B*, 2011, **176**, 727 – 735.
6 F. H. Lima and D. A. Cantane, in *Recent advances on nanostructured electrocatalysts for oxygen electro-reduction and ethanol electro-oxidation*, ed. F. L. de Souza and E. R. Leite, Springer Berlin Heidelberg, Berlin, Heidelberg, 2013, vol. 9783642317, pp. 125–151.
7 U. B. Demirci, *Journal of Power Sources*, 2007, **169**, 239–246.
8 A. Kowal, M. Li, M. Shao, K. Sasaki, M. B. Vukmirovic, J. Zhang, N. S. Marinkovic, P. Liu, A. I. Frenkel and R. R. Adzic, *Nature Materials*, 2009, **8**, 325–330.
9 J. Courtois, W. Du, E. Wong, X. Teng and N. A. Deskins, *Applied Catalysis A: General*, 2014, **483**, 85–96.
10 M. A. Akhairi and S. K. Kamarudin, *International Journal of Hydrogen Energy*, 2016, **41**, 4214–4228.
11 Y. Y. Hsia, Y. C. Huang, H. S. Zheng, Y. L. Lai, Y. J. Hsu, M. F. Luo and J. H. Wang, *Journal of Physical Chemistry C*, 2019, **123**, 11649–11661.
12 T. Sheng, C. Qiu, X. Lin, W. F. Lin and S. G. Sun, *Applied Surface Science*, 2020, **533**, 147505.
13 E. Antolini, *Journal of Power Sources*, 2007, **170**, 1–12.
14 F. Vigier, S. Rousseau, C. Coutanceau, J.-M. Leger and C. Lamy, *Topics in Catalysis*, 2006, **40**, 111–121.
15 Y. Zheng, X. Wan, X. Cheng, K. Cheng, Z. Dai and Z. Liu, *Catalysts*, 2020, **10**, 166.
16 J. Bai, D. Liu, J. Yang and Y. Chen, *ChemSusChem*, 2019, **12**, 2117–2132.

17 S. Ogo and Y. Sekine, *Fuel Processing Technology*, 2020, **199**, 106238.

18 M. Li, W. Guo, R. Jiang, L. Zhao, X. Lu, H. Zhu, D. Fu and H. Shan, *Journal of Physical Chemistry C*, 2010, **114**, 21493–21503.

19 P. Ferrin, D. Simonetti, S. Kandoi, E. Kunkes, J. A. Dumesic, J. K. Nørskov and M. Mavrikakis, *Journal of the American Chemical Society*, 2009, **131**, 5809–5815.

20 B. Schweitzer, S. N. Steinmann and C. Michel, *Physical Chemistry Chemical Physics*, 2019, **21**, 5368–5377.

21 Y. Choi and P. Liu, Catalysis Today, 2011, pp. 64–70.

22 J. J. Varghese and S. H. Mushrif, *React. Chem. Eng.*, 2019, **4**, 165–206.

23 M. Saleheen and A. Heyden, *ACS Catalysis*, 2018, **8**, 2188–2194.

24 C. D. Taylor and M. Neurock, *Current Opinion in Solid State and Materials Science*, 2005, **9**, 49 – 65.

25 G. Yang, L. Farsi, Y. Mei, X. Xu, A. Li, N. A. Deskins and X. Teng, *Journal of the American Chemical Society*, 2019, **141**, 9444–9447.

26 K. Mathew, R. Sundararaman, K.Letchworth-Weaver, T. A. Arias and R. G. Hennig, *J. Chem. Phys.*, 2014, **140**, 084106.

27 K. Mathew, V. S. C. Kolluru and R. G. Hennig, *VASPsol: Implicit solvation and electrolyte model for density-functional theory*, `https://github.com/henniggroup/VASPsol`, 2018, `https://github.com/henniggroup/VASPsol`.

28 M. Faheem, S. Suthirakun and A. Heyden, *The Journal of Physical Chemistry C*, 2012, **116**, 22458–22462.

29 A. Klamt and G. Schüürmann, *J. Chem. Soc., Perkin Trans. 2*, 1993, 799–805.

30 S. K. Iyemperumal and N. A. Deskins, *ChemPhysChem*, 2017, **18**, 2171–2190.

31 B. N. Zope, D. D. Hibbitts, M. Neurock and R. J. Davis, *Science*, 2010, **330**, 74–78.

32 C. J. Bodenschatz, S. Sarupria and R. B. Getman, *The Journal of Physical Chemistry C*, 2015, **119**, 13642–13651.

33 T. Xie, S. Sarupria and R. B. Getman, *Molecular Simulation*, 2017, **43**, 370–378.

34 C. Michel, F. Auneau, F. Delbecq and P. Sautet, *ACS Catalysis*, 2011, **1**, 1430–1440.

35 C. Hartnig, J. Grimminger and E. Spohr, *Electrochimica Acta*, 2007, **52**, 2236–2243.

36 M. Faheem and A. Heyden, *Journal of Chemical Theory and Computation*, 2014, **10**, 3354–3368.

37 H. H. Heenen, J. A. Gauthier, H. H. Kristoffersen, T. Ludwig and K. Chan, *The Journal of Chemical Physics*, 2020, **152**, 144703.

38 J. A. Herron, Y. Morikawa and M. Mavrikakis, *Proceedings of the National Academy of Sciences*, 2016, **113**, E4937—-E4945.

39 J. R. Pliego and J. M. Riveros, *Journal of Physical Chemistry A*, 2001, **105**, 7241–7247.

40 H.-F. Wang and Z.-P. Liu, *The Journal of Physical Chemistry C*, 2009, **113**, 17502–17508.

41 Y. M. Choi and P. Liu, *Journal of the American Chemical Society*, 2009, **131**, 13054–13061.

42 R. Alcalá, M. Mavrikakis and J. A. Dumesic, *Journal of Catalysis*, 2003, **218**, 178–190.

43 E. D. Wang, J. B. Xu and T. S. Zhao, *The Journal of Physical Chemistry C*, 2010, **114**, 10489–10497.

44 F. Colmati, G. Tremiliosi-Filho, E. R. Gonzalez, A. Berná, E. Herrero and J. M. Feliu, *Phys. Chem. Chem. Phys.*, 2009, **11**, 9114–9123.

45 E. A. Monyoncho, S. N. Steinmann, P. Sautet, E. A. Baranova and C. Michel, *Electrochimica Acta*, 2018, **274**, 274–278.

46 G. H. Gu, B. Schweitzer, C. Michel, S. N. Steinmann, P. Sautet and D. G. Vlachos, *The Journal of Physical Chemistry C*, 2017, **121**, 21510–21519.

47 M. Li, A. Kowal, K. Sasaki, N. Marinkovic, D. Su, E. Korach, P. Liu and R. R. Adzic, *Electrochimica Acta*, 2010, **55**, 4331–4338.

48 H. Idriss, *Platinum Metals Review*, 2004, **48**, 105–115.

49 G. Yang, A. I. Frenkel, D. Su and X. Teng, *ChemCatChem*, 2016, **8**, 2876–2880.

50 A. Resta, J. Blomquist, J. Gustafson, H. Karhu, A. Mikkelsen, E. Lundgren, P. Uvdal and J. N. Andersen, *Surface Science*, 2006, **600**, 5136–5141.

51 M. Li, A. Kowal, K. Sasaki, N. Marinkovic, D. Su, E. Korach, P. Liu and R. R. Adzic, *Electrochimica Acta*, 2010, **55**, 4331–4338.

52 M. Mavrikakis, J. Rempel, J. Greeley, L. B. Hansen, J. K. Nørskov and . J. Rempel, *The Journal of Chemical Physics*, 2002, **117**, 9901.

53 M. M. Yang, X. H. Bao and W. X. Li, *Journal of Physical Chemistry C*, 2007, **111**, 7403–7410.

54 J. Zhang, X. M. Cao, P. Hu, Z. Zhong, A. Borgna and P. Wu, *Journal of Physical Chemistry C*, 2011, **115**, 22429–22437.

55 B. Miao, Z.-P. Wu, H. Xu, M. Zhang, Y. Chen and L. Wang, *Computational Materials Science*, 2019, **156**, 175–186.

56 B. Miao, Z. Wu, H. Xu, M. Zhang, Y. Chen and L. Wang, *Chemical Physics Letters*, 2017, **688**, 92–97.

57 A. O. Pereira and C. R. Miranda, *Applied Surface Science*, 2014, **288**, 564–571.

58 N. Singh and C. T. Campbell, *ACS Catalysis*, 2019, **9**, 8116–8127.

59 J. Akinola, I. Barth, B. R. Goldsmith and N. Singh, *ACS Catalysis*, 2020, **10**, 4929–4941.

60 G. Kresse and J. Hafner, *Physical Review B*, 1994, **49**, 14251–14269.

61 G. Kresse and J. Hafner, *Physical Review B*, 1993, **47**, 558–561.

62 G. Kresse and J. Furthmüller, *Physical Review B - Condensed Matter and Materials Physics*, 1996, **54**, 11169–11186.

63 G. Kresse and J. Furthmüller, *Computational Materials Science*, 1996, **6**, 15–50.

64 S. Maintz, B. Eck and R. Dronskowski, *Computer Physics Communications*, 2011, **182**, 1421 – 1427.

65 M. Hacene, A. Anciaux-Sedrakian, X. Rozanska, D. Klahr, T. Guignon and P. Fleurat-Lessard, *Journal of Computational Chemistry*, 2012, **33**, 2581–2589.

66 M. Hutchinson and M. Widom, *Computer Physics Communications*, 2012, **183**, 1422–1426.

67 P. E. Blöchl, *Physical Review B*, 1994, **50**, 17953–17979.

68 G. Kresse and D. Joubert, *Physical Review B - Condensed Matter and Materials Physics*, 1999, **59**, 1758–1775.

69 J. P. Perdew, K. Burke and M. Ernzerhof, *Physical Review Letters*, 1996, **77**, 3865–3868.

70 M. Methfessel and A. T. Paxton, *Phys. Rev. B*, 1989, **40**, 3616–3621.

71 D. R. Lide, *CRC handbook of chemistry and physics*, CRC press, 2004, vol. 85.

72 C. J. Cramer, *Essentials of Computational Chemistry:Theories and Models, 2nd Edition*, Wiley, 2004.

73 V. Vorotnikov, S. Wang and D. G. Vlachos, *Industrial and Engineering Chemistry Research*, 2014, **53**, 11929–11938.

74 S. Sakong, M. Naderian, K. Mathew, R. G. Hennig and A. Groß, *The Journal of Chemical Physics*, 2015, **142**, 234107.

75 S. Behtash, J. Lu, E. Walker, O. Mamun and A. Heyden, *Journal of Catalysis*, 2016, **333**, 171–183.

76 Y. Sha, T. H. Yu, Y. Liu, B. V. Merinov and W. A. Goddard, *Journal of Physical Chemistry Letters*, 2010, **1**, 856–861.

77 T. Xie, C. J. Bodenschatz and R. B. Getman, *Reaction Chemistry and Engineering*, 2019, **4**, 383–392.

78 J. N. Brönsted, *Chemical Reviews*, 1928, **5**, 231–338.

79 R. P. Bell and C. N. Hinshelwood, *Proceedings of the Royal Society of London. Series A - Mathematical and Physical Sciences*, 1936, **154**, 414–429.

80 M. G. Evans and M. Polanyi, *Trans. Faraday Soc.*, 1938, **34**, 11–24.

81 S. Wang, B. Temel, J. Shen, G. Jones, L. C. Grabow, F. Studt, T. Bligaard, F. Abild-Pedersen, C. H. Christensen and J. K. Nørskov, *Catalysis Letters*, 2011, **141**, 370–373.

82 S. Wang, V. Petzold, V. Tripkovic, J. Kleis, J. G. Howalt, E. Skúlason, E. M. Fernández, B. Hvolbæk, G. Jones, A. Toftelund, H. Falsig, M. Björketun, F. Studt, F. Abild-Pedersen, J. Rossmeisl, J. K. Nørskov and T. Bligaard, *Physical Chemistry Chemical Physics*, 2011, **13**, 20760–20765.

83 J. E. Sutton and D. G. Vlachos, *ACS Catalysis*, 2012, **2**, 1624–1634.

84 J. Zaffran, C. Michel, F. Delbecq and P. Sautet, *Catal. Sci. Technol.*, 2016, **6**, 6615–6624.

85 Q. Zhang and A. Asthagiri, *Catalysis Today*, 2019, **323**, 35–43.

86 J. R. B. Gomes, F. Viñes, F. Illas and J. L. C. Fajín, *Phys. Chem. Chem. Phys.*, 2019, **21**, 17687–17695.

87 M. Mohsen-Nia, H. Amiri and B. Jazi, *Journal of Solution Chemistry*, 2010, **39**, 701–708.

88 C. Malmberg and A. Maryott, *Journal of Research of the National Bureau of Standards*, 1956, **56**, 1.

89 X. Zhang, R. S. DeFever, S. Sarupria and R. B. Getman, *Journal of Chemical Information and Modeling*, 2019, **59**, 2190–2198.

90 C. Michel, F. Göltl and P. Sautet, *Physical Chemistry Chemical Physics*, 2012, **14**, 15286–15290.

91 A. Fortunelli, W. A. Goddard, Y. Sha, T. H. Yu, L. Sementa, G. Barcaro and O. Andreussi, *Angewandte Chemie International Edition*, 2014, **53**, 6669–6672.

92 A. Fortunelli, W. A. Goddard III, L. Sementa and G. Barcaro, *Nanoscale*, 2015, **7**, 4514–4521.

93 S. Behtash, J. Lu, M. Faheem and A. Heyden, *Green Chemistry*, 2014, **16**, 605–616.

94 M. Valter, B. Wickman and A. Hellman, *The Journal of Physical Chemistry C*, 2021, **125**, 1355–1360.